

# Excitons of Composite Fermions

R.K. Kamilla, X.G. Wu, and J.K. Jain

*Department of Physics, State University of New York at Stony Brook, Stony Brook, New York*

*11794-3800*

(December 31, 2021)

## Abstract

The low-energy excitations of filled Landau levels (LL's) of electrons involve promotion of a single electron from the topmost filled LL to the lowest empty LL. These are called excitons or collective modes. The incompressible fractional quantum Hall states are understood as filled LL's of composite fermions, and the low-energy neutral excitations are excitons of composite fermions. New techniques are developed to study large systems, which provide detailed information about the dispersions of the composite fermion excitons. In particular, it is found that the interaction energy of the exciton is well described by the 'unprojected' composite fermion theory.

73.40.Hm

Typeset using REVTeX

---

<sup>0</sup>Accepted for publication in Physical Review B (1996).

## I. INTRODUCTION

The quantum Hall effect (QHE) is one of the most fascinating discoveries in physics in recent years. It concerns electron transport in two dimensional systems in the presence of a high transverse magnetic field. It has been found that there are plateaus on which the Hall resistance is quantized [1] at

$$R_H = \frac{h}{fe^2} \quad (1)$$

where  $f$  is either an integer or a simple fraction. For historical reasons, the observation of integer values of  $f$  is called the integer QHE (IQHE) and of fractional values of  $f$  is called the fractional QHE (FQHE). The longitudinal resistance in the plateau region is exponentially small, vanishing in the limit of temperature  $T \rightarrow 0$ .

Not long after the discovery of the FQHE, Laughlin [2] proposed the following wave function for the ground state at  $f = \frac{1}{(2m+1)}$ :

$$\psi_{1/(2m+1)} = \prod_{j < k} (z_j - z_k)^{2m+1} \exp[-\frac{1}{4} \sum_i |z_i|^2] \quad (2)$$

where  $z_j = x_j + iy_j$  denotes the coordinates  $(x_j, y_j)$  of the  $j$ th electron, and the lengths are expressed in unit of the magnetic length  $l_0 = \sqrt{\frac{\hbar c}{eB}}$ . This wave function was studied for small systems and found to be quite accurate. Laughlin also wrote trial wave functions for the charged excitations (quasielectrons and quasiholes, collectively referred to as quasiparticles).

Subsequently, Girvin, MacDonald and Platzman [3] (GMP) employed a single mode approximation (SMA) to investigate the neutral excitation of the Laughlin state, called the collective mode (CM) or exciton. The SMA takes the trial wave function of the collective excitation to be

$$\chi_k^{SMA} = \mathcal{P} \rho_k \psi_{1/(2m+1)} \quad (3)$$

where  $\mathcal{P}$  is the lowest-Landau-level (LLL) projection operator and

$$\rho_k = \sum_{j=1}^N e^{i\mathbf{k}\cdot\mathbf{r}_j} \quad (4)$$

is the density wave operator with wave vector  $k$ , which is the Fourier transform of the density

$$\rho(\mathbf{r}) = \sum_{j=1}^N \delta(\mathbf{r} - \mathbf{r}_j) , \quad (5)$$

for  $N$  electrons. The notation  $\chi$  will be used exclusively for the wave function of the collective mode or exciton in this article; the superscript will denote which scheme is used, and the subscript will show the quantum number. GMP evaluated the energy of this wave function, given by

$$\frac{\langle \chi_k^{SMA} | H - E_0 | \chi_k^{SMA} \rangle}{\langle \chi_k^{SMA} | \chi_k^{SMA} \rangle} , \quad (6)$$

as a function of  $k$ . In finite system studies, the SMA was found to work well in an intermediate range of wave vectors near a minimum in the dispersion, termed the “roton” minimum, in analogy with Feynman’s theory of superfluid  $^4\text{He}$  [4]. At wave vectors beyond the minimum, however, the SMA was not satisfactory. For large  $k$ , the energy of the true collective mode should be roughly independent of  $k$ , since it contains a far separated quasielectron-quasihole pair. The energy of  $\chi_k^{SMA}$ , however, continues to grow with  $k$ . Laughlin attempted an alternative description of the neutral collective mode in terms of a quasielectron-quasihole pair excitation [5]. This gave a reasonable description at large wave vectors, but did not produce the roton minimum. Thus, it was not possible to describe the full dispersion of the neutral excitation of  $f = 1/(2m + 1)$  in a single theoretical framework.

Much less was known about the collective modes of the other FQHE states. The SMA can be generalized to the other fractions as

$$\chi_k^{SMA} = \mathcal{P} \rho_k \psi_{n/(2mn+1)} , \quad (7)$$

where  $\psi_{n/(2mn+1)}$  is the incompressible ground state at  $f = \frac{n}{(2mn + 1)}$ . Since no good microscopic ansatz existed for  $\psi_{n/(2mn+1)}$ , the SMA was tested in finite system studies, with the exact numerical ground state used for  $\psi_{n/(2mn+1)}$  [6]. It, however, did not give a satisfactory description of the collective excitations [6]. Finite system exact diagonalization studies [7] also failed to provide a satisfactory overall picture for the collective excitations

at general fractions. The results showed a significant amount of finite size effects, making an extrapolation to the thermodynamic limit difficult.

In the last few years, there has been a resurgence of interest in this issue for two reasons. First, significant progress has been made on the experimental front. Pinczuk *et al.* [8] have measured the positions of the maxima and minima in the collective modes of the IQHE states, and recently also their dispersion in modulated density samples [9]. Further, Raman scattering [10] and phonon absorption [11] experiments have reported observation of the collective modes in the FQHE regime.

Secondly, there now exists a new theoretical framework, called the composite fermion (CF) theory [12], for describing all FQHE on an equal footing. The strongly correlated electrons are mapped on to weakly correlated composite fermions, which are electrons ‘dressed’ with  $2m$  vortices of the many particle wave function. They may be loosely thought of as electrons carrying  $2m$  flux quanta. The composite fermions experience a reduced effective magnetic field, and form energy levels, called CF-LL’s or quasi-LL’s, which are similar to the LL’s of electrons in this *reduced* magnetic field. The FQHE of electrons is understood as the IQHE of composite fermions, and the FQHE ground state at  $f = n/(2mn + 1)$  is interpreted as the state containing  $n$  filled CF-LL’s. The Laughlin wave function, in particular, is interpreted as one filled CF-LL. This description of the incompressible FQHE states suggests that the low-energy neutral excitations can be obtained by promoting a single composite fermion to the next higher CF-LL (Fig. 1), i.e., they are excitons of composite fermions. Their wave functions can be constructed in analogy to the wave functions of the excitons of electrons for IQHE states, and exact-diagonalization studies for systems containing up to 9 electrons have shown that they provide an extremely good quantitative description of the low-energy excitations of the FQHE states at  $1/3$ ,  $2/5$ , and  $3/7$  for all values of  $k$  accessible in these finite size systems [13,14].

The excited composite fermion will be called a quasielectron of the FQHE ground state, and the hole left behind a quasihole [15]. The essential difference between the SMA and the CF wave functions is that the SMA creates an *electron-hole* pair, whereas the CF wave

function creates a *quasielectron-quasihole* pair. We will see below that the SMA and the CF approaches are in general unrelated; the only exception is for the exciton at  $\frac{1}{(2m+1)}$ , for which the two become equivalent in the limit  $k \rightarrow 0$ .

Despite the confirmation of the validity of the CF scheme in small system studies, it has not been possible to study large systems yet. The main difficulty is that the CF wave functions have a small amount of mixing with higher LL's to begin with, and must be projected on to the lowest LL to obtain good quantitative estimates in the large  $B$  limit. The projection operator is quite complicated and no general computational schemes exist for dealing with it for large systems. In the present study, we develop two techniques for computing the properties of CF excitons for large systems. The first one computes the energy of the LLL-projected wave function of the CF exciton of the  $\frac{1}{(2m+1)}$  state by generalizing a method developed by Bonesteel [16]. This method, however, is inapplicable to other FQHE states. In the second one, we show that the 'unprojected' wave functions themselves can be used to a great extent for the study of the exciton dispersion. We have computed the (self) energy of a single quasielectron or quasihole in the unprojected scheme, and found it to be off by a factor of two to three [17]. However, the interaction between the quasielectron and quasihole participating in the exciton is found to be well described by the unprojected theory, except when they are very close. Therefore, the unprojected theory gives the exciton dispersion reasonably well up to an additive constant correcting for error in the self energies of the quasielectron and quasihole. We study large systems within the framework of the unprojected CF theory, and make qualitatively new and detailed predictions for various collective mode dispersions, which exhibit a rich structure with several minima. The extrema in the dispersion are of experimental relevance, since the CM density of states has peaks at the corresponding energies, which, as a result of a disorder-induced breakdown of the wave vector conservation, become observable in inelastic light scattering experiments [8].

The analogy to the IQHE excitons is helpful in explaining the number of minima and their positions. The relatively deep minima in the CM dispersion of the  $f = \frac{n}{(2mn+1)}$  FQHE state occur at approximately the same wave vector as those in the CM dispersion of

the  $f = n$  IQHE state. The latter originate from an interplay between the density profiles of the quasielectron in the  $(n + 1)$ th LL and the quasihole in the  $n$ th LL as they approach one another. Our study thus indicates that the wave function profile of the quasielectrons in the  $f = \frac{n}{(2mn + 1)}$  FQHE state is similar to that in the  $f = n$  IQHE state, further deepening the analogy between the FQHE and the IQHE implied by the CF theory.

The dispersions for the collective modes have also been calculated in a Chern-Simons (CS) field theoretical scheme in several recent papers. Here, the composite fermions are modeled as electrons carrying (gauge) flux quanta [12,18], which simulate vortices. The qualitative physical picture of composite fermions is obtained at a mean-field level, and a perturbation theory is carried out at the level of random-phase-approximation (RPA) [19]. Although the trial-wave-function and the CS schemes are both attempting to describe the same physics from different starting points, a precise relationship between them is not known at the moment. We will point out some similarities and differences between the results of the two methods in the specific context of the collective modes.

The plan of the paper is as follows. In Section II, we write the wave function of the CF exciton, and show that, for  $f = 1/(2m + 1)$ , it is equal to SMA wave function in the limit of small wave vectors. Section III gives the results of our study of the projected CF excitons, both in small systems, where a comparison with the exact results is possible, and in large systems, where Monte Carlo techniques [20,21] allow the computation of its dispersion for the 1/3 state. In Section IV, we study the interaction energy of the unprojected CF-exciton wave functions. It is shown that it provides a reasonably good quantitative description of the *interaction* between the quasielectron and the quasihole. Section V considers the analogy between the excitons of composite fermions, relevant for the FQHE, and those of electrons, relevant for the IQHE. This provides insight into the results of the previous sections, and also sheds light on the origin of the minima in the FQHE exciton dispersions. Section VI investigates the kinetic energies of the unprojected wave functions. It is shown to be less than the cyclotron energy for finite  $k$ , approaching the cyclotron energy as  $k \rightarrow 0$ . This is reminiscent of the Kohn's theorem, a weaker form of which is given for a class of wave

functions which are not eigenstates of any known Hamiltonian. The paper is concluded in Section VII. A short report of parts of this paper has been published elsewhere [22].

For future reference, here is a list of notations we will be using below for various wave functions and energies.

$\Phi_n$ : Slater determinant wave function of  $n$  filled LL's of electrons.

$\Phi_n^{CF}$  ( $\Phi_n^{UP-CF}$ ): Projected (unprojected) wave function of  $n$  filled LL's of composite fermions; this corresponds to the ground state of electrons at  $f = n/(2mn + 1)$ . The superscript 'UP' denotes 'unprojected'.

$\chi^{CF}$  ( $\chi^{UP-CF}$ ): Projected (unprojected) wave function of the CF exciton.

$\Delta V_{ex}$ : Exact energy of the exciton (measured relative to the exact ground state) from exact diagonalization in the lowest Landau level.

$\Delta V_p$ : Interaction energy of  $\chi^{CF}$  relative to  $\Phi^{CF}$ .

$\Delta V$  ( $\Delta K$ ): Interaction (kinetic) energy of  $\chi^{UP-CF}$  relative to  $\Phi^{UP-CF}$ .

## II. COMPOSITE FERMION EXCITONS

The basic principle of the CF theory [12] is that, in a range of filling factors, the electrons in the lowest LL find it energetically favorable to capture an even number of vortices of the many particle wave function. The bound state of an electron and the vortices behaves as a particle, called composite fermion. The vortices produce phases as the composite fermions move around, which partly cancel the Aharonov-Bohm phases originating from the external magnetic field, and, as a result, the composite fermions experience an effective magnetic field given by

$$B^* = B - 2m\rho\phi_0, \quad (8)$$

where  $B$  is the external field,  $2m$  is the number of vortices carried by composite fermions,  $\phi_0 = hc/e$  is the flux quantum, and  $\rho$  is the electron (or CF) density. The residual interaction between the composite fermions is weak, and the strongly correlated liquid of electrons maps

into a weakly interacting gas of composite fermions. An effective single-particle description of the electron state thus becomes possible in terms of composite fermions. The energy levels of composite fermions are analogous to the LL's of non-interacting electrons in this *weaker* magnetic field, and are called quasi- or CF-LL's. Defining the CF filling factor as  $\nu^* = \rho\phi_0/B^*$ , in analogy to the electron filling factor  $\nu = \rho\phi_0/B$ , the above equation can also be expressed as

$$\nu = \frac{\nu^*}{(2m\nu^* + 1)}. \quad (9)$$

The IQHE of composite fermions at  $\nu^* = n$  manifests as the FQHE of electrons at  $\nu = \frac{n}{(2mn + 1)}$ .

The trial wave functions for the CF states are constructed as follows. For simplicity, we confine our discussion to the special filling factors  $\nu = \frac{n}{(2mn + 1)}$ , which corresponds to the CF filling factor  $\nu^* = n$ . Let us denote the ground state of non-interacting electrons at  $\nu^* = n$  by  $\Phi_n$ . The wave function of  $n$  filled CF-LL's is obtained by attaching  $2m$  vortices to each electron in the state  $\Phi_n$ , which amounts to a multiplication by the Jastrow factor

$$D^m \equiv \prod_{j < k} (z_j - z_k)^{2m}, \quad (10)$$

which produces

$$\Phi_n^{UP-CF} = \prod_{j < k} (z_j - z_k)^{2m} \Phi_n. \quad (11)$$

This wave function is not strictly in the lowest LL (although it is largely so [23]), and must be projected on to the LLL to obtain a wave function appropriate to the limit  $B \rightarrow \infty$ :

$$\Phi_n^{CF} = \mathcal{P}\Phi_n^{UP-CF}. \quad (12)$$

$\Phi_n^{CF}$  describes the electron ground state at  $\nu = \frac{n}{(2mn + 1)}$ . It has been tested for several FQHE states in small system exact calculations and found to be extremely accurate [13,14].

Armed with this analogy between the IQHE and the FQHE states, we are now in a position to write a wave function for the CF exciton (or the CF collective mode). It is



obtained from the exciton of the  $\nu = n$  IQHE state precisely in the same manner as the FQHE ground state is obtained from the  $\nu = n$  IQHE ground state, i.e., by multiplication by the Jastrow factor, followed by LLL projection:

$$\chi_k^{CF} = \mathcal{P}\chi_k^{UP-CF}, \quad (13)$$

where

$$\chi_k^{UP-CF} = \prod_{j<k} (z_j - z_k)^{2m} \rho_k^{n \rightarrow n+1} \Phi_n \quad (14)$$

Here,  $\rho_k^{n \rightarrow n+1} \Phi_n$  is the exciton of the  $\nu = n$  state. In this wave function, a single electron has been excited from the  $n^{\text{th}}$  LL of  $\Phi_n$  to the  $(n+1)^{\text{th}}$  LL, creating an exciton whose kinetic energy is equal to the cyclotron energy at the reduced magnetic field,  $\hbar\omega_c^* = \frac{\hbar\omega_c}{(2mn+1)}$  [24]. By analogy,  $\chi^{CF}$  contains a single excited composite fermion in the  $(n+1)^{\text{th}}$  CF-LL and a hole left behind in the  $n^{\text{th}}$  CF-LL, as shown schematically in Fig. 1.

The SMA wave function for the collective mode at  $\nu = \frac{1}{(2m+1)}$  has a CF-type interpretation, as it is obtained from  $\rho_k \Phi_1$  after multiplication by the Jastrow factor and then projecting the product on to the lowest LL. We now show that the CF and the SMA wave functions become identical in the limit of  $k \rightarrow 0$  for this mode. This follows because, in general, in the limit  $k \rightarrow 0$ ,

$$\rho_{k \rightarrow 0} \Phi_n = \rho_{k \rightarrow 0}^{n \rightarrow n+1} \Phi_n. \quad (15)$$

To see this, we express  $\rho_k$  and  $\rho_k^{n \rightarrow n+1}$  in the second quantized form. Denote the single particle states by  $|p, s\rangle$ , where  $p$  is the wave vector quantum number and  $s = 0, 1, \dots$  is the LL index (note that the topmost occupied LL of  $\Phi_n$  is  $s = n - 1$ ). The explicit form of the wave function in the Landau gauge is given by

$$\phi_{p,s} = (2\pi 2^s s! \sqrt{\pi})^{-1/2} \exp[ipy - \frac{1}{2}(x+p)^2] H_s(x+p), \quad (16)$$

where  $H_s$  is the Hermite polynomial, and the magnetic length has been set equal to unity. In the second quantized notation, the density operator is given by

$$\rho_k = \sum_{p,p',s,s'} a_{p's'}^\dagger a_{ps} \langle p's' | e^{iky} | ps \rangle \quad (17)$$

where the y-axis has been chosen parallel to the wave vector  $k$ . In the present case, we have  $s < n$  and  $s' \geq n$  since  $\rho_k$  is applied to a state with  $n$  filled LL's. Aside from an overall normalization factor, it is given by, for  $s' > s$ ,

$$\rho_k = \sum_{s,s'} (2^{s+s'} s! s'!)^{-1/2} e^{-k^2/4} 2^{-s} s! k^{s'-s} L_s^{s'-s}(k^2/2) \int dp a_{p+k,s'}^\dagger a_{ps} . \quad (18)$$

The operator  $\rho_k^{n \rightarrow n+1}$  is given by the term with  $s = n - 1$  and  $s' = n$ . Eq. (15) follows in the limit  $k \rightarrow 0$ . For fractions other than  $\nu = 1/(2m + 1)$ ,  $\chi^{SMA}$  does not have a CF-type interpretation, and  $\chi^{CF}$  and  $\chi^{SMA}$  are different at all  $k$ .

### III. PROJECTED WAVE FUNCTION

This section investigates the projected CF wave function. The spherical geometry [25,26] is used in all our calculations, where  $N$  electrons move on the surface of a sphere under the influence of a radial magnetic field. The flux through the surface is  $2q\phi_0$ , where  $2q$  is an integer. The single particle eigenstates are called monopole harmonics,  $Y_{q,\ell,\ell_z}$ , where  $\ell = |q|, |q| + 1, \dots$  is the single particle angular momentum, and  $\ell_z = \pm\ell, \pm\ell - 1, \dots$  is the z-component of  $\ell$ . The total orbital angular momentum  $L$  of the many body system is related to the wave vector of the planar geometry by  $kl_0 = \frac{L}{\sqrt{q}}$  [26]. In the spherical geometry the energy separation between the  $n^{th}$  and the  $(n + 1)^{th}$  LL is given by  $\left(1 + \frac{n}{q}\right) \frac{\hbar e B}{mc}$ , which reduces to the usual cyclotron energy in the limit  $q \rightarrow \infty$ . We find it more convenient to use as our unit of the kinetic energy  $\hbar\omega_c \equiv \left(1 + \frac{1}{q}\right) \frac{\hbar e B}{mc}$ , the separation between the lowest two LL's.

If the highest occupied LL shell in  $\Phi_n$  has angular momentum  $\ell$ , then the IQHE exciton has a single excited electron in the  $(n + 1)^{th}$  LL, with angular momentum  $\ell + 1$ , and the hole in the  $n^{th}$  LL, with angular momentum  $\ell$ . The Slater determinant basis states can be denoted by

$$|\ell_z^e, \ell_z^h \rangle$$

where  $\ell_z^e$  ( $\ell_z^h$ ) is the z-component of the angular momentum of the electron in the  $(n+1)^{th}$  LL (hole in the  $n^{th}$  LL). The allowed values of  $L$  for the exciton are  $L = 1, 2 \dots 2\ell + 1$ , with precisely one multiplet at each  $L$ , containing  $2L + 1$  degenerate states. The  $k = 0$  in the planar geometry corresponds to  $L = 1$  in the spherical geometry, which is the smallest  $L$  possible for the exciton. With no loss of generality, we restrict our calculations below to the sector with  $L_z = 0$ , with the understanding that each state in this sector represents  $2L + 1$  degenerate states of the full Hilbert space. The exciton wave function  $\rho_L^{n \rightarrow n+1} \Phi_n$  is a *unique* linear superposition of the Slater determinant basis states, given by (with  $L_z = 0$ )

$$\rho_L^{n \rightarrow n+1} \Phi_n = \sum_{\ell_z = -\ell}^{\ell} \langle \ell + 1, \ell_z; \ell, -\ell_z | L, 0 \rangle | \ell_z, -\ell_z \rangle, \quad (19)$$

The wave function of the CF exciton at the corresponding  $L$ ,  $\chi_L^{CF}$ , is obtained by multiplication by the Jastrow factor, as in Eq. (13). The Jastrow factor in the spherical geometry is  $\Phi_1^2$ , where  $\Phi_1$  is the wave function of the lowest filled LL, multiplication by which does not change the  $L$  of the state. Clearly,  $\chi_L^{CF}$  *also does not contain any adjustable parameters*.

We have computed the exciton energy using the projected CF wave function  $\chi^{CF}$ , denoted by  $\Delta V_p$ , for finite systems. It is measured relative to the projected CF ground state energy. Our brute force projection method (see Ref. [14] for details) allows us to carry out the projection for general states only for up to 8-9 electrons, which severely limits the size of the systems for which  $\Delta V_p$  may be evaluated.

Figs. 2 and 3 give the actual Coulomb energies,  $\Delta V_{ex}$ , obtained by an exact numerical diagonalization of the Hamiltonian, along with the energies of the projected CF wave functions. First note that the range over which the exciton extends in the exact diagonalization studies agrees with that predicted by the CF theory. (A state exists at  $L = 1$  for the IQHE exciton, but it is annihilated by the projection operator while constructing the wave function for the CF exciton.)  $\Delta V_p$  is within a few percent of the exact energy  $\Delta V_{ex}$ .

For the exciton at  $\nu = 1/3$ , we have obtained  $\Delta V_p$  for large systems using variational Monte Carlo, which relies on the special feature of  $\chi^{UP-CF}$  that it contains no more than one electron in the second LL, and none at all in the higher LL's. This follows since the IQHE

exciton wave function,  $\rho_k^{1 \rightarrow 2} \Phi_1$ , has only one electron in the second LL, and multiplication by the Jastrow factor does not promote electrons to higher LL's. The projected wave function can then be written as [16]

$$\chi^{CF} \propto (K - \hbar\omega_c)\chi^{UP-CF} \quad (20)$$

where, we remind the reader that  $\hbar\omega_c = (1 + \frac{1}{q})\hbar\frac{eB}{mc}$ . The kinetic energy operator  $K$ , in standard notation is given by

$$K = \frac{\hbar\omega_c}{2q} \sum_{j=1}^N \left[ -\frac{1}{\sin\theta_j} \left( \frac{\partial}{\partial\theta_j} \left( \sin\theta_j \frac{\partial}{\partial\theta_j} \right) \right) + \frac{1}{\sin^2\theta_j} (q \cos\theta_j - m_j)^2 \right] - \frac{N}{2}\hbar\omega_c \quad (21)$$

where our choice of the gauge (or, 'section' [25]) is defined by  $i\partial_\phi Y_{q,\ell,\ell_z} \equiv (q - \ell_z)Y_{q,\ell,\ell_z}$ , and the kinetic energy is measured relative to the LLL. Each Slater determinant is updated at every step of the Monte Carlo following the method of Ref. [21], which takes  $\mathcal{O}(N^2)$  operations. The computation of the energy is rather involved and time consuming not only due to the presence of derivatives in the expression of  $K$ , but also from the fact that  $\chi^{UP-CF}$  is a linear superposition of  $\sim \mathcal{O}(N)$  Slater determinants, necessitating  $\mathcal{O}(N^3)$  operations for updating the determinants at each step. It should also be mentioned that the computation of the interaction energy of  $\chi^{CF}$  is much more stable when  $|\chi^{UP-CF}|^2$ , rather than  $|\chi^{CF}|^2$ , is chosen as the Monte Carlo weight function.

The CF-exciton energy is shown as a function of  $L$  for a 20 electron system in Fig. 4. Computation of each point takes approximately 5-6 days of computer time on the IBM RISC 6000 workstation. The  $k \rightarrow 0$  ( $L = 1$ ) energy,  $0.15e^2/\epsilon l_0$ , is consistent with the SMA prediction. There is a deep minimum at the expected position of  $kl_0 \approx 1.4$ . From Fig. 5, the estimate for the thermodynamic value of the energy at the minimum is  $0.063(3)e^2/\epsilon l_0$ , which should be compared to the SMA prediction  $0.078e^2/\epsilon l_0$  [3]. We note here that the same wave function for the ground state (the Laughlin wave function) is used in both the CF and the SMA calculations.

Two additional minima are clearly visible at  $kl_0 \approx 2.7$  and  $kl_0 \approx 3.5$ . Are they real? We believe so. A direct confirmation of the genuineness of the minimum at  $kl_0 \approx 2.7$  is

seen in the nine-electron exact diagonalization calculation of Fano *et al.* [27], reproduced in Fig. 6(c). (The exact diagonalization systems are too small to see the third minimum.) We note that there is no principle that rules out the existence of more than one minimum in the dispersion of the  $1/3$  exciton; the structure here arises simply from an interplay between the structures in the density profiles of the quasielectron and quasihole, as the distance between them is varied. This will be discussed later in greater detail.

We note that the exciton energy predicted by the projected CF theory may not be very accurate in the limit  $k \rightarrow 0$ , as indicated by the following considerations. (i) The LLL projection of the unprojected state becomes small and vanishes as  $k \rightarrow 0$  (i.e., at  $L = 1$ ), suggesting that the act of projection may not be as innocuous here as at larger  $k$ . (ii) It was found in small system calculations that  $\chi^{CF}$  does not exhaust the oscillator strength at small wave vectors to the same extent as it does at larger  $k$  [13,14]. This was attributed to the fact that the exciton branch comes quite close to the higher bands at small  $k$ ; the exact state mixes with higher band states to reduce its energy, whereas any such mixing is neglected in the CF approach. (For  $2/5$  and  $3/7$ , the CF description continues to work up to the smallest wave vectors available in the finite size studies.) (iii) In the SMA theory, the  $k \rightarrow 0$  energy of the  $1/3$  collective mode was close to twice the energy at the minimum. Our somewhat improved estimate shows that the ratio between the two energies is definitely greater than two, approximately 2.4. This suggests that the actual lowest energy excitation at small  $k$  may contain *two* pairs of CF-excitons — these will have a more complicated quadrupolar structure [3,28]. A better understanding of the nature of the low-energy excitations in the small- $k$  limit would require further investigation.

For other fractions,  $\Phi^{UP-CF}$  and  $\chi^{UP-CF}$  have a finite fraction of electrons in higher LL's, and the above method for the LLL projection is not useful. Below, we use a different approach which, though less accurate, can be applied to the excitons of other FQHE states as well.

#### IV. UNPROJECTED CF EXCITON: INTERACTION ENERGY

It has been known that the unprojected CF wave functions already reside mostly in the lowest LL [23], with very small kinetic energies per particle. It is natural to ask if they can be used, without projection, for the computation of various quantities. This has been addressed for the charge gap (relevant for transport), equal to the energy required to create a far separated quasielectron-quasihole pair, which is nothing but an exciton at a large  $k$ . It was found that the gap computed with the unprojected wave functions was smaller than the projected gap by as much as a factor of 2-3 [17]. This may suggest that the unprojected wave functions are not relevant for a quantitative understanding.

Fortunately, this turns out not to be the case. We will see in this section that the interaction energy of  $\chi^{UP-CF}$  is close to the energy of  $\chi^{CF}$ , up to an overall additive constant, except at very small  $k$ . In other words, if the interaction energy of  $\chi^{UP-CF}$  is called  $\Delta V$  (measured relative to the unprojected CF ground state), then  $\Delta V + \Gamma$  provides a good approximation to the exciton dispersion, except at small  $k$ . The constant  $\Gamma$  can be fixed by requiring the large  $k$  limit to equal the transport gap (which is experimentally measurable). The underlying physics will be discussed in the next section.

We first test this assertion in finite system calculations. The energy  $\Delta V + \Gamma$  (with a suitable choice of  $\Gamma$ ) is shown in Figs. 6 and 7 for finite systems, where  $\Delta V$  is computed by variational Monte Carlo. It indeed captures the essential features of  $\Delta V_{ex}$ ; in particular, it obtains correctly the minima and maxima. It also provides a good quantitative approximation for the exciton energy: it is quite accurate for 1/3, and reasonably accurate (to within 15-20%) for 2/5 and 3/7 (for which the agreement improves with the system size).

The advantages of working with the unprojected CF wave functions are that a treatment of large systems becomes possible, and that all FQHE states can be considered. Fig. 4 gives the dispersion ( $\Delta V + \Gamma$ , where  $\Gamma = 0.064e^2/\epsilon l_0$  is obtained from the extrapolation of finite system values) for a 20-electron system for the 1/3 FQHE state. A lack of any significant size dependence for systems with slightly larger  $N$  shows that these results are close to

the thermodynamic limit. Let us first concentrate on the range  $kl_0 > 0.5$ . Here,  $\Delta V + \Gamma$  provides a good approximation for  $\Delta V_p$ . A deep minimum appears at the expected position  $kl_0 \approx 1.4$ . The other two minima at  $kl_0 \approx 2.7$  and  $kl_0 \approx 3.5$  are also seen in  $\Delta V$ , although they are less pronounced than in  $\Delta V_p$ .  $\Delta V$  also underestimates the size of the structure in Fig. 7, which seems to be a general feature.

$\Delta V + \Gamma$  is shown in Fig. 8 for  $1/3$ ,  $2/5$  and  $3/7$  for large systems, with  $\Gamma$  suitably chosen to produce a reasonable large- $k$  limit. The positions of the two deep minima for the  $2/5$  exciton agree well with those found in the exact diagonalization results of [6], as also does the feature that the second minimum is deeper. The relatively complicated structure in the dispersion clarifies why the small system calculations are unable to provide a coherent picture.

A curious feature of the exciton dispersion in Fig. 4 is that  $\Delta V$  bends downward at small wave vectors ( $kl_0 < 0.5$  for  $1/3$ ). The unprojected scheme is not trustworthy here, since LL mixing becomes a more serious problem here. (Remember, at  $L = 1$ ,  $\chi^{UP-CF}$  has a zero projection on the lowest LL [13]). Indeed,  $\Delta V_p$  for  $1/3$  shows no such bending.

## V. ANALOGY TO IQHE

An insight into the above results can be gained from a comparison with the exciton of the  $\nu^* = n$  IQHE state [24].

### A. positions of minima

First we consider the number of minima and their positions. Fig. 9 shows the exciton dispersion of the IQHE states at  $\nu^* = 1, 2$  and  $3$ . These have one, two and three minima (some of these are relative to a rising background, and appear as inflection points), respectively, which corresponds exactly to the number of strong minima in the exciton dispersions for  $1/3, 2/5$  and  $3/7$ . To pursue this analogy further, we have shown by arrows the positions ( $L$ ) of the minima/inflection points of the corresponding IQHE state in the dispersions of

Figs. 2– 7 (in each case, the IQHE state with the same  $N$  has been used to determine the minima). For the  $1/3$  state, this obtains the  $L$  of the minimum off by one unit (which is an insignificant error in the thermodynamic limit) while for  $2/5$  and  $3/7$ , it predicts the positions of minima correctly. Given that  $L = kl_0\sqrt{q}$ , and  $l_0^{-1} \propto \sqrt{B} \propto \sqrt{q}$ , this implies that the minima occur at the same  $k$  for the FQHE and IQHE states related by the CF theory.

### B. Interaction energy of CF exciton

The exciton contains a quasihole and a quasielectron. For sufficiently large  $k$ , when the quasiparticles are far apart, the energy of the CF exciton can be thought of as having three contributions: the self energy of the quasielectron (which is the energy to create an isolated quasielectron), the self energy of the quasihole, and the interaction energy between them. The interaction energy is a monotonic function of the distance between the quasiparticles, proportional to  $1/r$ , when they are far apart. As they approach one another, there is a non-monotonic, oscillatory contribution to the interaction energy originating from the fact that the quasiparticles are not point-like objects but have a finite extent, with oscillatory structure in their density profiles. At very small  $k$ , when the size of the exciton becomes of the order of the size of a single quasiparticle, the distinction between the self and interaction energies becomes nebulous, and the above intuitive picture breaks down.

As mentioned earlier, the unprojected CF theory is not able to predict the self energies of the quasiparticles quantitatively. However, these do not have any  $k$  dependence, and can be corrected by an additive constant  $\Gamma$ . The results of the previous section show that the unprojected CF approach does a good job of estimating the *interaction* energy of the quasihole and quasielectron, with is responsible for the structure in the exciton dispersion.

So long as the interaction energy is small compared to the self energy, the densities of the constituent quasiparticles are not much affected. The structure in the interaction energy then arises largely from the structure in the density profiles of the individual quasiparticles.



This motivates us to ask if the unprojected CF theory gives a reasonable description of the density profiles of the quasiparticles. To this end, we first investigate if the FQHE quasiparticles have any relation to the IQHE quasiparticles. The simplest case is of the quasidelectron and quasihole of the  $\frac{1}{(2m+1)}$  state. These are related, respectively, to the quasidelectron and quasihole of the  $\nu^* = 1$  state, i.e., to states with the LLL completely occupied except for a hole, and the LLL completely occupied plus an additional electron in the second LL. The associated densities are given by

$$\frac{\rho(r)}{\rho_0} = 1 - e^{-\frac{1}{2}r^2} , \quad (22)$$

and

$$\frac{\rho(r)}{\rho_0} = 1 + \frac{1}{2}r^2 e^{-\frac{1}{2}r^2} , \quad (23)$$

respectively, where  $\rho_0 = (2\pi l_0^2)^{-1}$  is the density of the filled LL. These are plotted in Fig. 10. The density profiles are different simply because the hole is in the LLL, while the additional electron resides in the second LL. The analogy to the IQHE thus provides a natural explanation of the asymmetry between the quasihole and quasidelectron. The charge densities of the quasihole and the quasidelectron of the Laughlin  $1/3$  state [30] are similar to those in Fig. 10. In particular, the quasidelectron of the  $1/3$  state has a smoke-ring shape with a dip at the origin. The maximum of the quasidelectron of the  $\nu^* = 1$  state is at  $r = \sqrt{2} l_0$ . This predicts a maximum for the  $1/3$  quasidelectron at  $r = \sqrt{6} l_0$  (since the  $l_0$ 's at  $\nu = 1$  and  $\nu = 1/3$  differ by a factor of  $\sqrt{3}$ ), which is in excellent agreement with  $r \approx \sqrt{6} l_0$  found in earlier studies [30]. The value of  $\rho/\rho_0$  at the origin is 1.0 and that at the maximum is  $1 + e^{-1} = 1.37$ , which should be compared to  $\rho/\rho_0 \approx 0.93$  and  $\rho/\rho_0 \approx 1.26$  (where  $\rho_0$  now is the electron density of the  $1/3$  state), respectively, for the  $1/3$  quasidelectron (taken from Morf and Halperin [30]). The quasiholes at  $\nu = 1/3$  and  $\nu = 1$  also have rather similar shapes, except near the origin. The similarity between the quasiparticles of a FQHE state, which are completely determined by interactions between electrons confined to the lowest LL, with the quasiparticles of the corresponding IQHE state, governed by the LL physics,

is quite impressive. This appearance of the higher-LL-like structure within the lowest LL is an explicit illustration of the basic principles of the CF theory. The wave functions of the quasiparticles of other FQHE states are expected to have more complicated profiles, since the radial part of the single particle wave function in higher LL's has several nodes.

Multiplication by the Jastrow factor does not change the main features of the IQHE quasiparticles, although it introduces additional weaker oscillations. It was seen in Ref. [16] that  $\chi^{UP-CF}$  gives a good description of the density profile even in the region of overlap between the quasielectron and quasihole.

### C. Small $k$ limit

Another feature of the unprojected results is that  $\Delta V$  decreases for small  $k$  (apparently vanishing as  $k \rightarrow 0$ ). This can again be understood by analogy to the IQHE collective modes, for which also the interaction energy vanishes in the limit  $k \rightarrow 0$ , as guaranteed by the Kohn's theorem [31].

The analogy between the FQHE and the IQHE excitons is, of course, not true in every detail. In particular, it applies only to the strong structure. There are weaker minima in the CF exciton dispersion, which have no analog in the dispersion of the corresponding IQHE exciton. These appear only after multiplication by the Jastrow factor (with or without the LLL projection), and thus refer to very fine features beyond the mean-field theory. These are related to weaker oscillations in the density profiles of the FQHE-quasiparticles that are not seen for the corresponding IQHE-quasiparticles. Also, the relative strengths of the strong minima do not necessarily correspond to those in the IQHE dispersion. For example, at  $\nu^* = 2$ , the second minimum is much weaker than the first one (Fig. 9), unlike at  $\nu = 2/5$  where the first one is weaker (Fig. 8).

The principal minimum for the  $1/3$  collective mode has been interpreted as a precursor of the Wigner crystal instability [3]. The above interpretation is cast in terms of the IQHE of composite fermions. A reconciliation between the two should prove interesting.

## VI. UNPROJECTED CF MODE: KINETIC ENERGY

Further insight into some features of the above results can be gained by considering the kinetic energy of the various unprojected wave functions. We emphasize that it has no direct relevance to the actual energy of the collective mode (at least in the limit of large  $B$ ), except that it must be sufficiently small in order for the LLL projection to retain the important correlations of the CF theory.

The kinetic energy of the IQHE exciton (measured relative to the ground state) is precisely  $\hbar\omega_c^*$ . We consider here the kinetic energy  $\Delta K$  of the CF exciton, defined as

$$\Delta K = \frac{\langle \chi^{UP-CF} | K - E_0 | \chi^{UP-CF} \rangle}{\langle \chi^{UP-CF} | \chi^{UP-CF} \rangle}, \quad (24)$$

where

$$E_0 = \frac{\langle \Phi_n^{UP-CF} | K | \Phi_n^{UP-CF} \rangle}{\langle \Phi_n^{UP-CF} | \Phi_n^{UP-CF} \rangle}, \quad (25)$$

and  $K$  is the kinetic energy operator. The kinetic energy per electron for the ground state,  $E_0/N$ , is known to be small [23].

Before coming to numerical calculations, we mention an exact result. It was proved earlier that the rigorous upper limit for  $\Delta K$  for  $\nu = 1/(2m + 1)$  is the cyclotron energy, since  $\chi^{UP-CF}$  cannot have more than one electron in the second LL. It has also been shown earlier that at  $L = 1$ , the wave function has zero projection on to the lowest LL, indicating that it has at least one electron in the second LL [7,13]. Taken together, one concludes that  $\chi^{UP-CF}$  has precisely one electron in the second LL at  $L = 1$ , i.e., its energy approaches the cyclotron energy in the limit  $k \rightarrow 0$ . For other fractions, no exact results are known.

$\Delta K$  cannot be evaluated analytically in general. We have computed it by two methods. For small systems, we expand  $\chi^{UP-CF}$  and  $\Phi^{UP-CF}$  in the Slater determinant basis. For  $\chi^{UP-CF}$ , there are a total of 18,814 basis states for  $N = 7$  at  $\nu = 1/3$  (in the  $L_z = 0$  subspace, allowing a maximum of one electron in the second LL), and 4,448,884 basis states for  $N = 8$  at  $\nu = 2/5$  (in the  $L_z = 0$  subspace, allowing for a maximum of four electrons in

the second and one electron in the third LL). The amplitudes of various basis states can be obtained by an elaborate book-keeping. Despite the large basis sizes, we are able to evaluate  $\Delta K$  exactly (numerically) for these systems (Fig. 11), since it is not necessary to store the amplitudes of all states. In these calculations, we put by hand the LL spacing to be the same for all consecutive LL's. As expected,  $\Delta K$  of the 1/3 state at  $L = 1$  is exactly equal to the cyclotron energy. For 2/5 also,  $\Delta K$  at  $L = 1$  is close to  $\hbar\omega_c$  as seen in Fig. 11(b). The actual values for  $\Delta K/\hbar\omega_c$  at  $L = 1$  for 4, 6, and 8 electrons are 1.0219, 1.0091, and 1.0050, respectively, approaching unity approximately as  $1 + 0.9N^{-5/2}$ .

We have studied bigger systems by Monte Carlo, and the results are shown in Fig. 12.  $\Delta K$  is small, less than the cyclotron energy in the entire  $k$  range for all FQHE states. It approaches  $\hbar\omega_c$  as  $k \rightarrow 0$ , in accordance with the Kohn's theorem (below). At large  $k$ , its value is equal to the kinetic energy of a far separated quasielectron-quasihole pair. For the 1/3 state, the large- $k$  limit is equal to  $0.16 \hbar\omega_c$ , which is also the kinetic energy of an isolated quasielectron [23] (since the quasihole is strictly in the lowest LL in this case). For the 2/5 and 3/7 states,  $\Delta K$  shows 2 and 3 shallow minima respectively which occur at approximately the same positions as the minima in  $\Delta V^{UP-CF}$ , demonstrating that  $\Delta K$  also shares some qualitative features of the true exciton dispersion. Also note that  $\Delta K$  increases at small  $k$ , which sheds light on why the results obtained in previous sections become questionable here.

As discussed earlier, the SMA wave function for the collective mode at 1/3 is obtained by CF transformation from the state  $\rho_k \Phi_1$ . The kinetic energy of this wave function is given by

$$\frac{\langle \Phi_1 | \rho_k^\dagger (K - E_0) \rho_k | \Phi_1 \rangle}{\langle \Phi_1 | \rho_k^\dagger \rho_k | \Phi_1 \rangle} . \quad (26)$$

Substituting from Eq. (18), this is equal to

$$\frac{\sum_{m=1}^{\infty} m S(m)}{\sum_{m=1}^{\infty} S(m)} \hbar\omega_c^* , \quad (27)$$

with  $S(m) = 2^m m! k^{2m}$ , where we have used the fact that  $L_0^m(x) = 1$  for arbitrary  $x$ . This yields the kinetic energy of  $\rho_k \Phi_1$  to be

$$\frac{k^2/2}{1 - e^{-k^2/2}} \hbar\omega_c^* . \quad (28)$$

It approaches the cyclotron energy in the limit  $k \rightarrow 0$ , as expected from Kohn's theorem. As  $k$  increases, however, the kinetic energy of  $\rho_k \Phi_1$  increases, as shown in Fig. 13 (solid line), indicating an increasing occupation of higher LL's. Clearly, it is not an appropriate wave function for the exciton of the  $\nu = 1$  IQHE state. The SMA wave function thus has a large occupation of higher CF LL's at large  $k$ . Fig. 13 also shows (squares) the kinetic energy of the 'unprojected SMA wave function',  $\prod_{j < k} (z_j - z_k)^2 \rho_k \Phi_1$ , measured relative to the kinetic energy of the state  $\prod_{j < k} (z_j - z_k)^2 \Phi_1$ , for 20 electrons. It approaches  $\hbar\omega_c$  as  $k \rightarrow 0$  for the same reason as  $\Delta K$  (also see, He *et al.* [7]), but increases rapidly beyond  $kl_0 \approx 1.5$ .

Before closing the Section, we state a generalization of the Kohn's theorem, which sheds light on the feature seen above that the kinetic energy of the unprojected wave functions approaches  $\hbar\omega_c$  in the limit of  $k \rightarrow 0$  for all FQHE states. The Kohn's theorem states that for any given *eigenstate*  $\Psi$ , with eigenvalue  $E$ ,  $a_0^\dagger \Psi$  is also an eigenstate with eigenvalue  $E + \hbar\omega_c$ , with

$$a_0^\dagger \equiv \sum_{i=1}^N a_i^\dagger , \quad (29)$$

where  $a_i^\dagger$  is the LL raising operator. The unprojected CF wave functions, however, are not eigenstates of the Hamiltonian (in particular of the kinetic energy). A weaker form of Kohn's theorem applies to a class of wave functions which are not eigenstates of the Hamiltonian. More specifically,

$$\frac{\langle a_0^\dagger \Psi | H - E | a_0^\dagger \Psi \rangle}{\langle a_0^\dagger \Psi | a_0^\dagger \Psi \rangle} = \hbar\omega_c, \quad (30)$$

where  $H = K + V$  and  $E = \langle \Psi | H | \Psi \rangle / \langle \Psi | \Psi \rangle$ , provided that  $\Psi$  can be written in a factorized form

$$\Psi = \Phi \zeta_{COM} \quad (31)$$

where (i)  $\Phi$  does not depend on the center-of-mass (COM) coordinates, (ii)  $\zeta_{COM}$  depends *only* on the COM coordinates, and (iii)  $\zeta_{COM}$  is an eigenstate of the COM kinetic energy.

All these properties are satisfied by any eigenstate. This generalized Kohn's theorem can be proven straightforwardly by transforming to the center of mass and relative coordinates, and noting that there is no mixing between the COM and relative coordinates in the kinetic energy  $K$ , which is a sum of two parts, one containing only the COM coordinate and the other containing only the relative coordinates. The operators  $a_0^\dagger$  and  $a_0$  are recognized as the LL raising and lowering operators for the COM coordinate. The theorem then follows since the application of  $a_0^\dagger$  changes the kinetic energy by precisely  $\hbar\omega_c$ , but leaves the interaction energy unchanged (since it is independent of the COM coordinate).

The unprojected CF wave function for the incompressible FQHE state at  $\nu = n/(2n+1)$  is given by

$$D^m \Phi'_n \exp\left[-\frac{1}{4} \sum_{i=1}^N |z_i|^2\right] , \quad (32)$$

where the prime on  $\Phi'_n$  denotes that the exponential has been factored out. To see that it has the same form as the wave functions in Eq. (30), note that the exponential can be expressed as

$$\exp\left[-\frac{1}{4} \left( \sum_{i=1}^{N-1} (z_i - \eta_0)(z_i^* - \eta_0^*) + \left| \sum_{i=1}^{N-1} (z_i - \eta_0) \right|^2 \right)\right] \exp\left[-\frac{N}{4} \eta_0 \eta_0^*\right] , \quad (33)$$

where  $\eta_0 = N^{-1} \sum_{j=1}^N z_j$  is the COM coordinate. The factor  $D^m \Phi'_n$  is independent of the COM coordinates, since it is invariant under the replacement  $z_j \rightarrow z_j - \eta_0$ . The COM coordinate thus factors out; in fact,  $\zeta_{COM} = \exp\left[-\frac{N}{4} \eta_0 \eta_0^*\right]$  is a ground state of the COM kinetic energy.

These considerations provide a systematic way of constructing new trial states at the same energy and also at energies differing by  $\hbar\omega_c$ , by using the angular momentum and LL raising operators of the COM coordinate. This is related to the fact, seen routinely in finite size studies, that once an eigenenergy appears at any angular momentum value, it appears at all larger angular momenta as well [32,33].

## VII. CONCLUSION

In short, the following unified picture becomes possible in the CF framework: the incompressible ground states contain an integer number of filled CF-LL's and the excited states are obtained by exciting composite fermions to higher CF-LL's. Not surprisingly, the same physics provides the key to understanding both the ground state and its excitations.

We have carried out a detailed study of the neutral excitations of the  $1/3$ ,  $2/5$  and  $3/7$  states and developed techniques that allow us to deal with fairly large systems. Predictions have been made for the rich structure of the collective modes of various FQHE states. The dispersion of the  $\frac{n}{(2n+1)}$  state has  $n$  strong minima, and several additional weaker minima. The strong minima can be explained by analogy to the IQHE, and appear at the same wave vector as the minima in the collective modes of the IQHE states. The weaker minima, on the other hand, have no analog in the FQHE. The existence of these structures has been corroborated, whenever possible, with the help of exact diagonalization study.

There is qualitative agreement between the results of our calculations and those of the Chern-Simons theory. The latter also obtains flat dispersion at large  $k$ , several minima, and finite energy in the limit  $k \rightarrow 0$ . A quantitative comparison is not as good, however. A crucial feature of the CS scheme is that, at small  $k$ , the mode derived from the  $n \rightarrow n+1$  IQHE mode is pushed up to the cyclotron energy due to the RPA screening. This may be related to the feature discovered in Section VI that  $\Delta K \rightarrow \hbar\omega_c$  as  $k \rightarrow 0$  for the unprojected CF wave function. A better understanding of these and other issues will require further work.

Several effects left out in the above study must be incorporated before a comparison with experiment may be made. Modification in the Coulomb interaction due to the finite width of the quantum well [34], LL mixing [35], and disorder [5,36] are all known to change the numerical values of the excitation energies. We believe that a good first approximation for the experimental CM dispersion can be obtained by  $\Delta V + \Gamma$ , with a choice of  $\Gamma$  that makes the large- $k$  limit equal to the experimental transport gap.

This work was supported in part by the National Science Foundation under Grant no. DMR93-18739. It is a pleasure to acknowledge valuable discussions with S.A. Kivelson, A.H. MacDonald, and A. Pinczuk.



## REFERENCES

- [1] K. von Klitzing, G. Dorda and M. Pepper, Phys. Rev. Lett. **45**, 494 (1980); D.C. Tsui, H.L. Stormer and A.C. Gossard, Phys. Rev. Lett. **48**, 1559 (1982).
- [2] R.B. Laughlin, Phys. Rev. Lett. **50**, 1395 (1983).
- [3] S.M. Girvin, A.H. MacDonald and P.M. Platzman, Phys. Rev. Lett. **54** 581, 1985; Phys. Rev. B **33**, 2481 (1986).
- [4] *Statistical Mechanics* by R.P. Feynman (Benjamin Reading, Mass. 1972).
- [5] R.B. Laughlin, Physica **126 B**, 254 (1985).
- [6] W.P. Su and Y.K. Wu, Phys. Rev. B **36**, 7565 (1987).
- [7] S. He, S.H. Simon and B.I. Halperin, Phys. Rev. B **50**, 1823 (1994).
- [8] A. Pinczuk *et al.*, Phys. Rev. Lett. **61**, 2701 (1988).
- [9] L.L. Sohn *et al.*, Solid State Commun. **93**, 897 (1995).
- [10] A. Pinczuk *et al.*, Phys. Rev. Lett. **70** 3983, 1993; Semiconductor Science and Technology, vol. **9**, 1865 (1994).
- [11] C.J. Mellor *et al.*, Phys. Rev. Lett. **74**, 2339 (1995).
- [12] J.K. Jain, Phys. Rev. Lett. **63**, 199 (1989); Phys. Rev. B **41**, 7653 (1990); Science **266**, 1199 (1994).
- [13] G. Dev and J.K. Jain, Phys. Rev. Lett. **69**, 2843 (1992).
- [14] X.G. Wu and J.K. Jain, Phys. Rev. B **51**, 1752 (1995).
- [15] A.S. Goldhaber and J.K. Jain, Phys. Lett. A **199**, 267 (1995).
- [16] N.E. Bonesteel, Phys. Rev. B **51**, 9917 (1995).
- [17] X.G. Wu, R.K. Kamilla, and J.K. Jain, unpublished.

- [18] A. Lopez and E. Fradkin, Phys. Rev. B **44**, 5246 (1991).
- [19] A. Lopez and E. Fradkin, Phys. Rev. B **47**, 7080 (1993); S.H. Simon and B.I. Halperin, Phys. Rev. B **48**, 17368 (1993); *ibid.*, **50**,1807 (1994); S. He, S.H. Simon and B.I. Halperin, Phys. Rev. B **50**, 1823 (1994); X.C. Xie, *ibid.*, **49**, 16833 (1994); L. Zhang, *ibid.*, **51**, 4645 (1995); and Phys. Rev. B, in print (SISSA preprint no. cond-mat/9506113).
- [20] *Monte Carlo Methods in Statistical Physics*, edited by K. Binder (Springer-Verlag, NY 1979), and references therein; Monte Carlo Simulations of Disordered Systems, by S. Jain (World Scientific, Singapore 1992).
- [21] D. Ceperley, G.V. Chester, M.H. Kalos; Phys. Rev. B **16**, 3081 (1977); S. Fahy, X.W. Wang, and S.G. Louie, Phys. Rev. B **42**, 3503 (1990).
- [22] R.K. Kamilla, X.G. Wu, and J.K. Jain, Phys. Rev. Lett. **76**, 1332 (1996).
- [23] N. Trivedi and J.K. Jain, Mod. Phys. Lett. B **5**, 503 (1991).
- [24] C. Kallin and B.I. Halperin, Phys. Rev. B **30**, 5655 (1984); and the references therein.
- [25] T.T. Wu and C.N. Yang, Nucl. Phys. B **107**, 365 (1976); T.T. Wu and C.N. Yang, Phys. Rev. D **16**, 1018 (1977).
- [26] See, F.D.M. Haldane in *The Quantum Hall Effect*, edited by R.E. Prange and S.M. Girvin (Springer-Verlag, NY 1990).
- [27] G. Fano, F. Ortolani and E. Colombo, Phys. Rev. B **34**, 2670 (1986).
- [28] D.H. Lee and S.C. Zhang, Phys. Rev. Lett. **66**, 1220 (1991).
- [29] N. d'Ambrumenil and R. Morf, Phys. Rev. B **40**, 6108 (1989).
- [30] E.g., see R. Morf and B.I. Halperin, Phys. Rev. B **33**, 2221 (1986).
- [31] W. Kohn, Phys. Rev. B **123**, 1242 (1961).

- [32] S.A. Trugman and S. Kivelson, Phys. Rev. B **31**, 5280 (1985).
- [33] M. Stone, H.W. Wyld, and R.L. Schult, Phys. Rev. B **45**, 14156 (1992).
- [34] F.C. Zhang and S. Das Sarma, Phys. Rev. B **33**, 2903 (1986); D. Yoshioka, J. Phys. Soc. Jpn. **55**, 885 (1986).
- [35] D. Yoshioka, J. Phys. Soc. Jpn. **53**, 3740 (1984); X. Zhu and S.G. Louie, Phys. Rev. Lett. **70**, 339 (1993) V. Melik-Alaverdian and N.E. Bonesteel, Phys. Rev. B **52**, R17032 (1996); Rodney Price and S. Das Sarma, preprint.
- [36] A.H. MacDonald, A.H. Liu, S.M. Girvin and P.M. Platzman, Phys. Rev. B **33**, 4014 (1986), S.M. Girvin in *The Quantum Hall Effect*, edited by R.E. Prange and S.M. Girvin (Second Edition, Springer-Verlag, NY 1990).

FIGURES

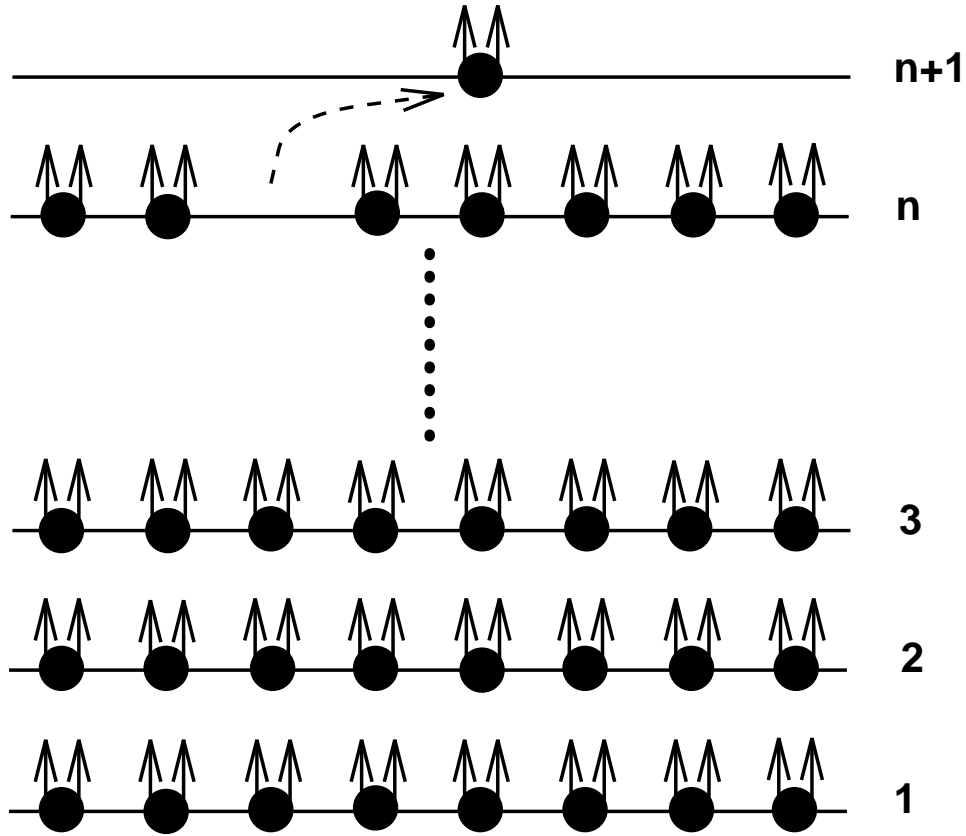


FIG. 1. Schematic view of a CF exciton. Each filled circle with two arrows depicts a composite fermion as an electron carrying two flux quanta. All composite fermions on a given line are in the same CF Landau level. A CF exciton of the  $n$  filled CF-LL state [which corresponds to  $\nu = n/(2n+1)$  FQHE state of electrons] is obtained by promoting a single composite fermion from the topmost occupied [ $n$ th] CF Landau level to the lowest unoccupied [ $(n+1)$ th] CF Landau level.

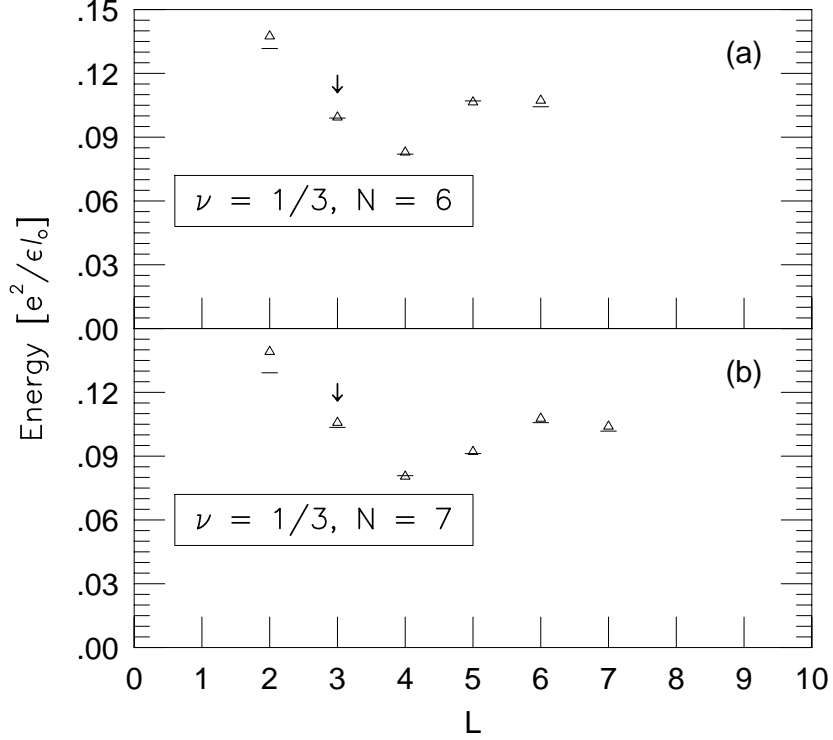


FIG. 2. The exact energies  $\Delta V_{ex}$  (dashes) and projected CF energies  $\Delta V_p$  (triangles) are shown for the exciton of the 1/3 state for systems of 6 and 7 particles. All interaction energies here and in the following curves are in units of  $e^2/\epsilon l_0$ , where  $l_0$  is the magnetic length, and  $\epsilon$  is the background dielectric constant. The arrows here and in the following figures indicate the angular momenta at which minima or inflection points occur in the exciton dispersion for the corresponding filled LL IQHE state ( $\nu = 1$  state in this figure) for the same  $N$ . The energy of the ground state at  $L = 0$  has been set to zero.

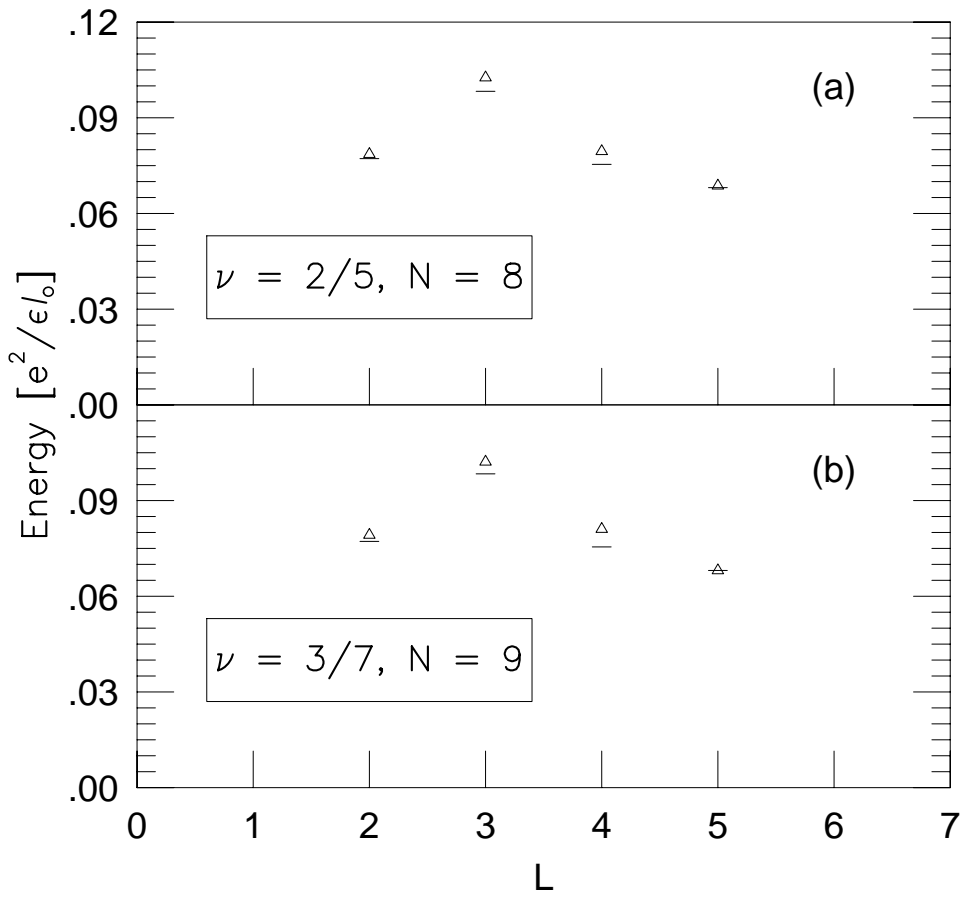


FIG. 3. Same as Fig. 2 for the exciton at  $\nu = 2/5$  and  $3/7$ .

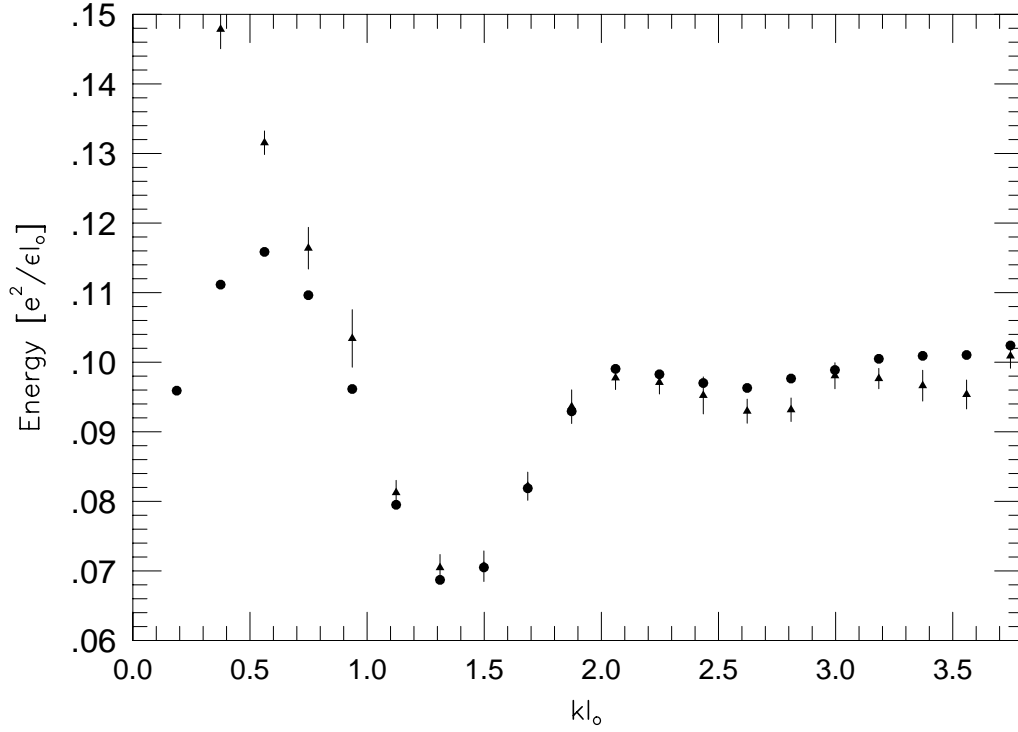


FIG. 4.  $\Delta V + \Gamma$  with  $N = 20$  and  $\Gamma = 0.064e^2/\epsilon l_0$  (filled circles); and  $\Delta V_p$  (filled triangles) for 1/3 CF state.  $\Delta V_p$  ( $\Delta V$ ) is the interaction energy of the projected (unprojected) CF state. The statistical errors of Monte-Carlo estimation of the energies are shown on each point for the projected energy; in the case of the unprojected energies the error is of the order of the size of the filled circles.

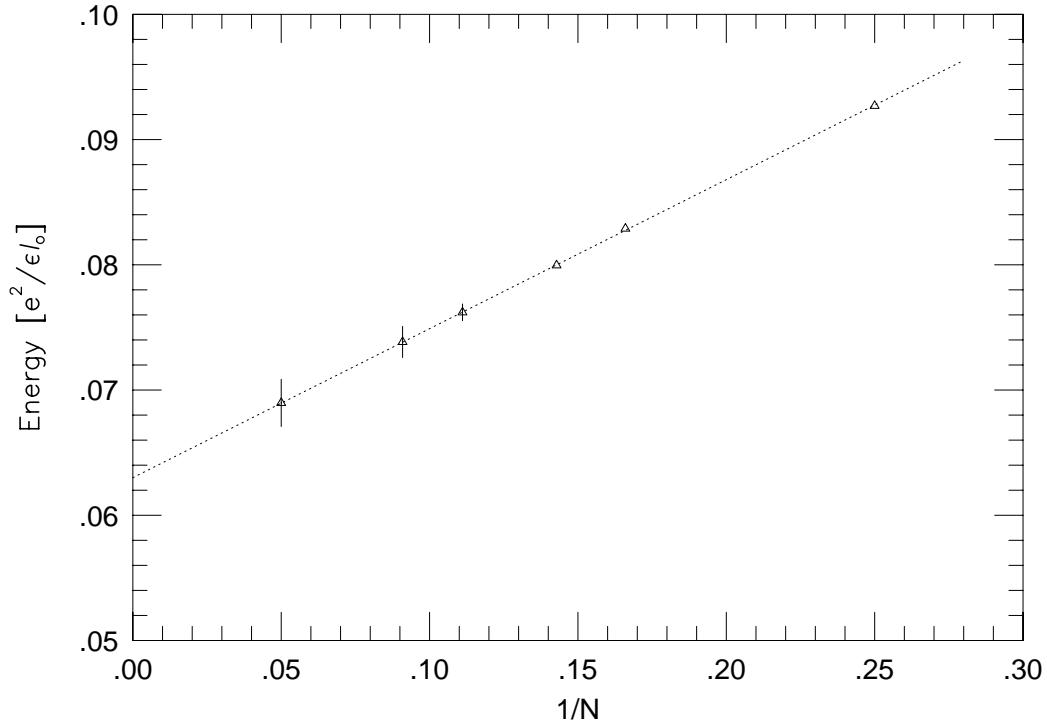


FIG. 5. Estimation of  $\Delta V_p$  at the minimum of the exciton dispersion at  $\nu = 1/3$ . For each value of  $N$ , the minimum was determined by smooth polynomial interpolation in the neighborhood of the minimum to reduce the sensitivity of our thermodynamic estimation to the discreteness of  $L$  for finite systems. A linear  $\chi^2$ -fit gives a thermodynamic estimate of  $0.063 e^2/\epsilon l_0$ , with an uncertainty of 2 (3) in the last digit if four (three) largest systems are used.



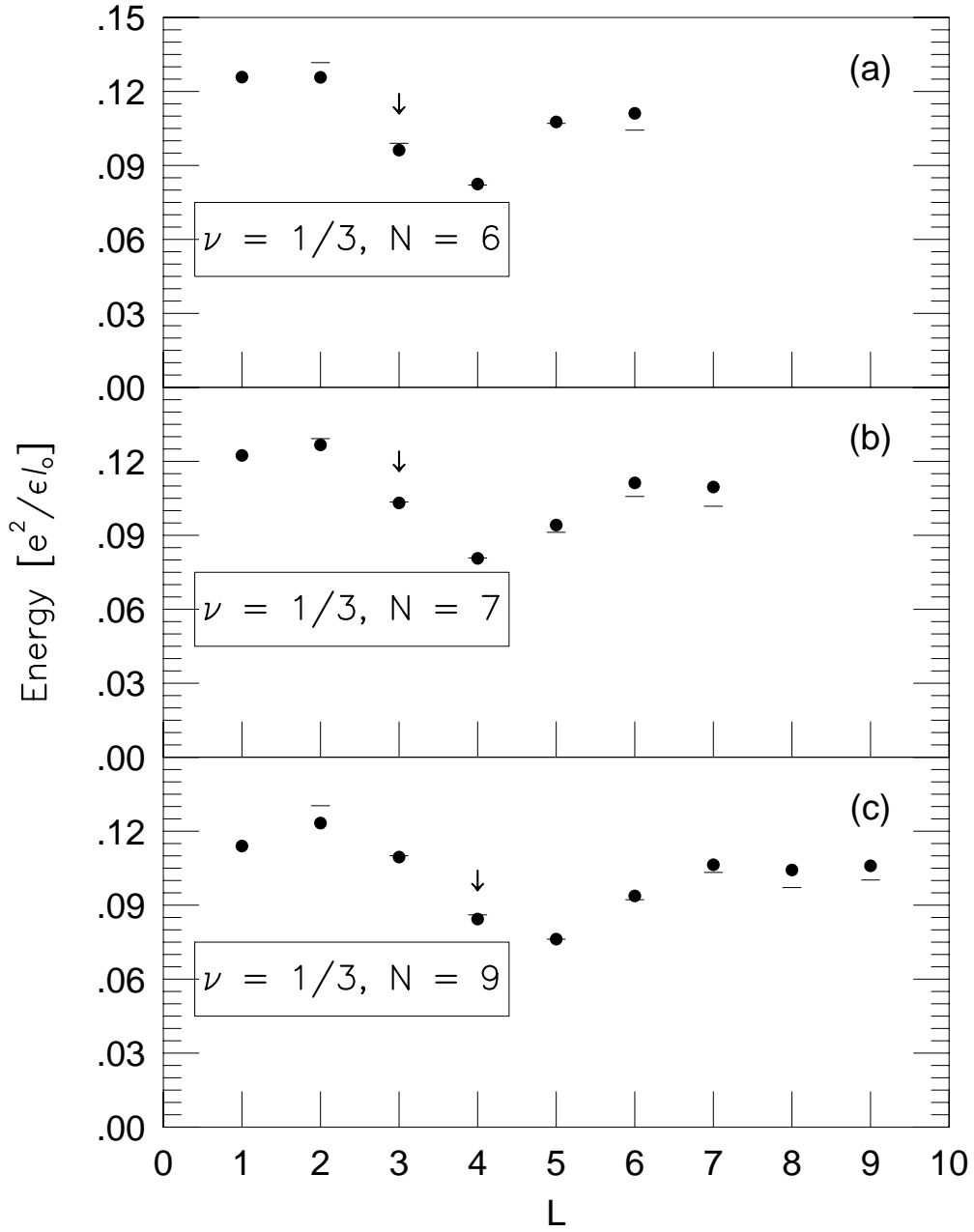


FIG. 6. The exact energies  $\Delta V_{ex}$  (dashes) and  $\Delta V + \Gamma$  (filled circles) are shown for the exciton of the  $1/3$  state for systems of 6, 7 and 9 particles.  $\Gamma$  is chosen so as to match the two energies at the minimum. The exact energies in (c) are taken from Fano *et al.* [27].

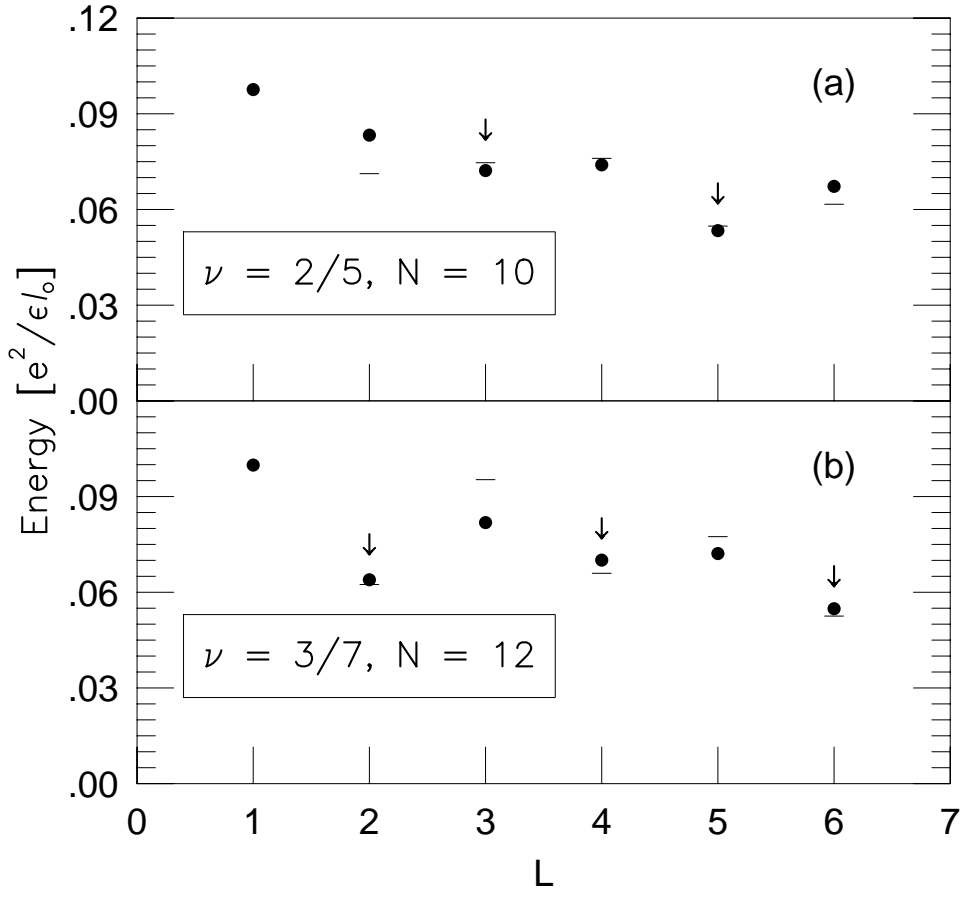


FIG. 7. Same as Fig. 4 for the 2/5 and 3/7 state. The exact energies in (a) are taken from d'Ambrumenil and Morf [29] and in (b) from He *et al.* [19].

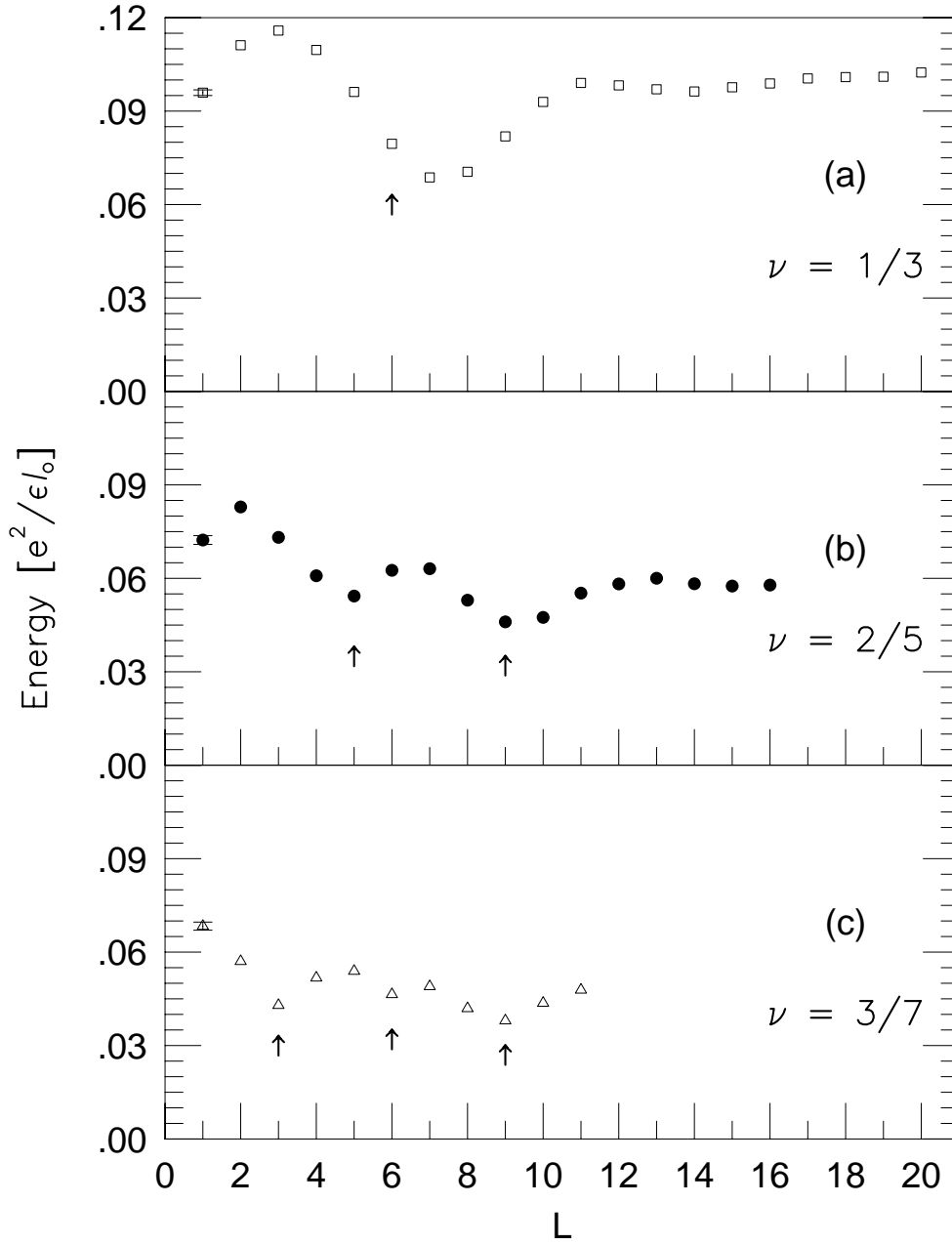


FIG. 8.  $\Delta V + \Gamma$  is shown for (a)  $\nu = 1/3$ ,  $N = 20$ ,  $\Gamma = 0.064e^2/\epsilon l_0$ ; (b)  $\nu = 2/5$ ,  $N = 30$ ,  $\Gamma = 0.037e^2/\epsilon l_0$ ; and (c)  $\nu = 3/7$ ,  $N = 27$ ,  $\Gamma = 0.028e^2/\epsilon l_0$ . The typical error bar is shown on the first point in each case.

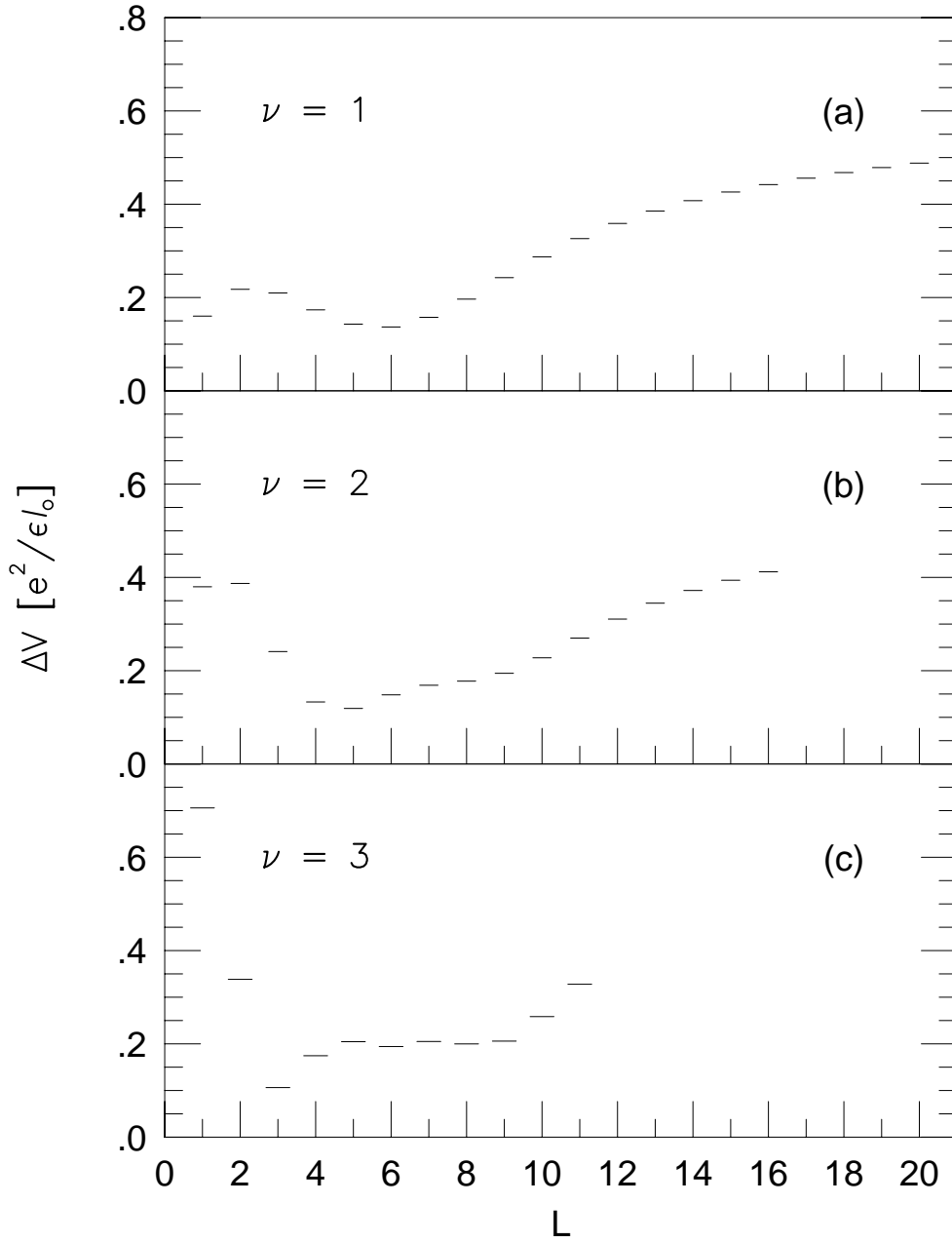


FIG. 9.  $\Delta V$  for lowest energy exciton of (a)  $\nu = 1$ ,  $N = 20$ , (b)  $\nu = 2$ ,  $N = 30$ , and (c)  $\nu = 3$ ,  $N = 27$ . These correspond to the FQHE systems in Fig. 8. There are  $n$  minima/inflection points in the lowest branch of the collective mode of the  $\nu = n$  IQHE state.

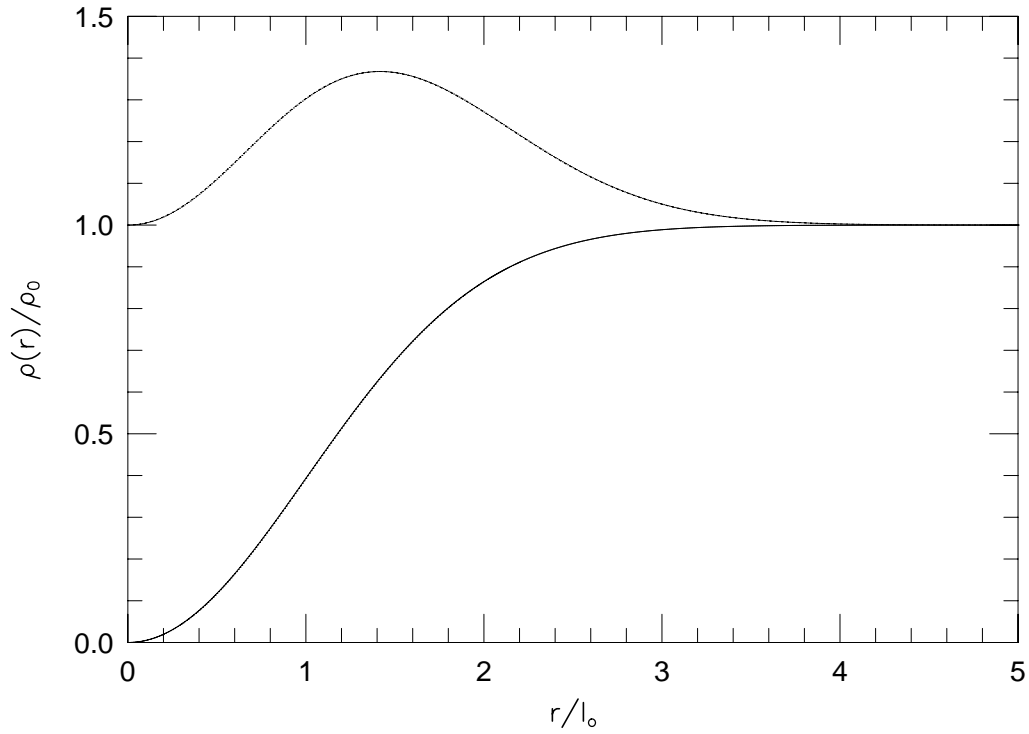


FIG. 10. The charge density of the (a)  $\nu = 1$  quasihole (solid line), which is the fully occupied lowest LL except for a hole at the origin, and (b)  $\nu = 1$  quasielectron (dashed line), which is the fully occupied lowest LL plus an electron in the second LL at the origin.

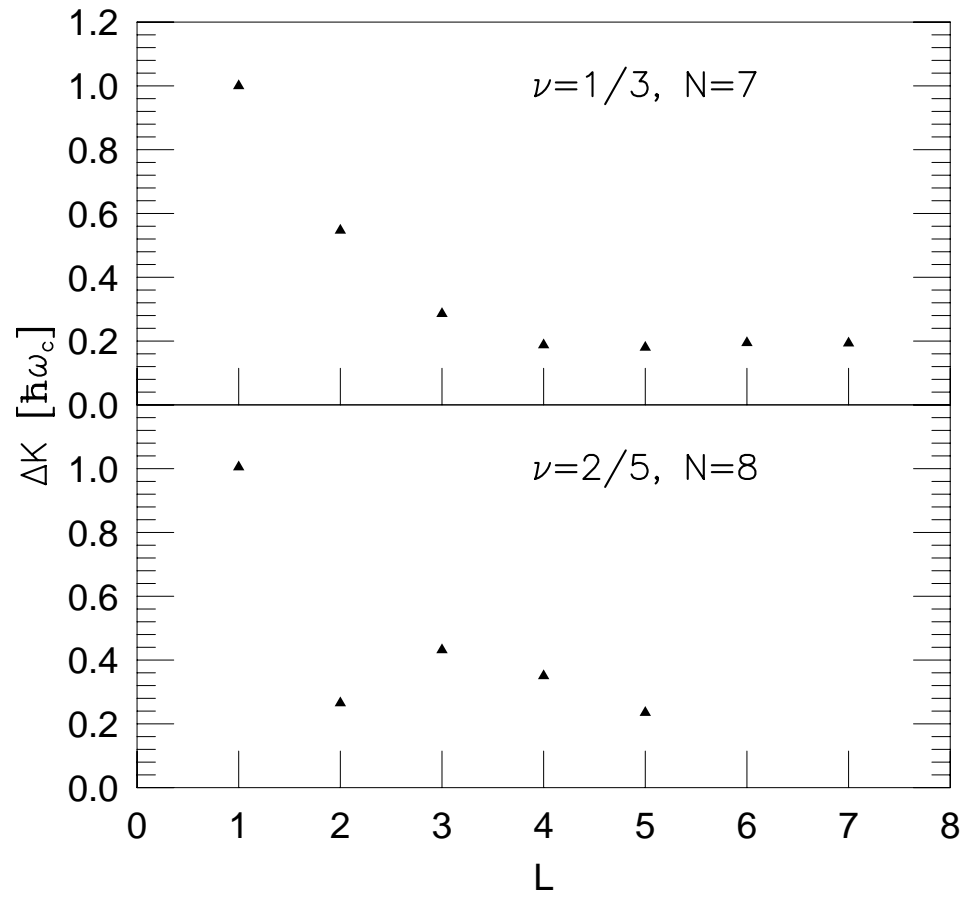


FIG. 11. Exact  $\Delta K$  for (a)  $\nu = 1/3$ ,  $N = 7$ ; (b)  $\nu = 2/5$ ,  $N = 8$ .

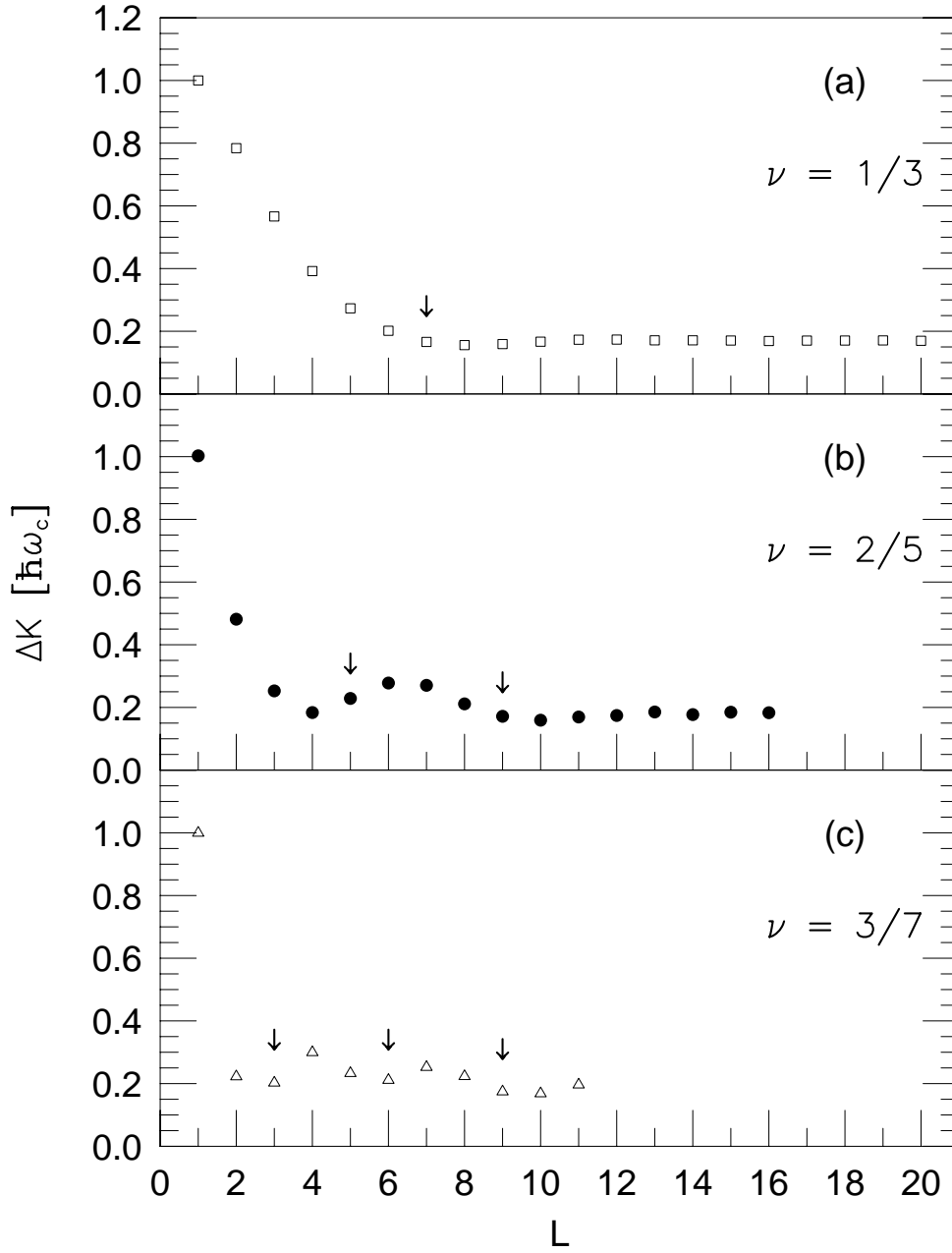


FIG. 12. Monte Carlo estimate for  $\Delta K$  using the unprojected CF exciton wave function for (a)  $1/3$  state of 20 particles, (b)  $2/5$  state of 30 particles, and (c)  $3/7$  state of 27 particles. The statistical error is smaller than the size of the symbol used.

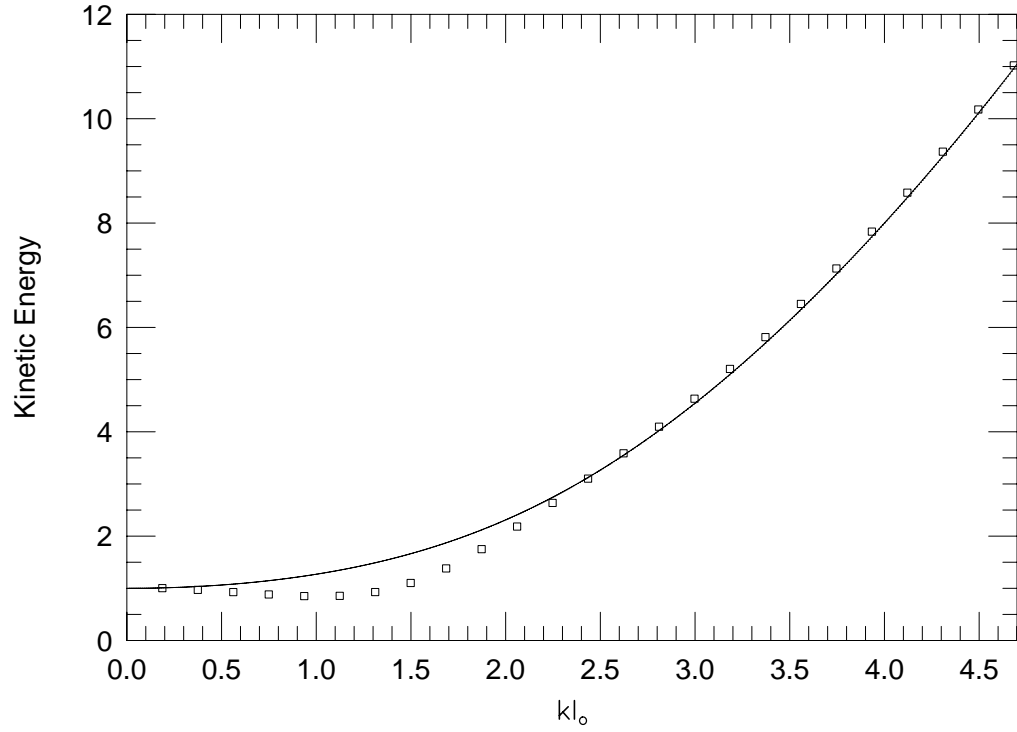


FIG. 13. The kinetic energy of the ‘unprojected SMA state’, in units of  $\hbar\omega_c$ , for the collective mode of the  $1/3$  state ( $N = 20$ ), shown by squares. The solid line plots Eq. (28) in unit of  $\hbar\omega_c^*$ .